Biochimica et Biophysica Acta 1848 (2015) 2918–2931

Contents lists available at ScienceDirect

Biochimica et Biophysica Acta

journal homepage: www.elsevier.com/locate/bbamem

Human lactoferricin derived di-peptides deploying loop structures induce apoptosis specifically in cancer cells through targeting membranous phosphatidylserine☆

Sabrina Riedl [a,*], Regina Leber [a], Beate Rinner [b], Helmut Schaider [c,d], Karl Lohner [a,e], Dagmar Zweytick [a,*]

[a] Institute of Molecular Biosciences, Biophysics Division, NAWI Graz, University of Graz, Humboldtstraße 50/III, A-8010 Graz, Austria
[b] Center for Medical Research, Medical University of Graz, Stiftingtalstraße 24, A-8010 Graz, Austria
[c] Cancer Biology Unit, Department of Dermatology, Medical University of Graz, Auenbruggerplatz 8, A-8036 Graz, Austria
[d] Dermatology Research Centre, Translational Research Institute, School of Medicine, The University of Queensland, Brisbane, Queensland, Australia
[e] BioTechMed-Graz, Austria

ARTICLE INFO

Article history:
Received 20 April 2015
Received in revised form 10 July 2015
Accepted 30 July 2015
Available online 1 August 2015

Keywords:
Antitumor peptides
Apoptosis
Phosphatidylserine
Melanoma
Glioblastoma
Targeted therapy

ABSTRACT

Host defense-derived peptides have emerged as a novel strategy for the development of alternative anticancer therapies. In this study we report on characteristic features of human lactoferricin (hLFcin) derivatives which facilitate specific killing of cancer cells of melanoma, glioblastoma and rhabdomyosarcoma compared with non-specific derivatives and the synthetic peptide RW-AH. Changes in amino acid sequence of hLFcin providing 9–11 amino acids stretched derivatives LF11-316, -318 and -322 only yielded low antitumor activity. However, the addition of the repeat (di-peptide) and the retro-repeat (di-retro-peptide) sequences highly improved cancer cell toxicity up to 100% at 20 μM peptide concentration. Compared to the complete parent sequence hLFcin the derivatives showed toxicity on the melanoma cell line A375 increased by 10-fold and on the glioblastoma cell line U-87mg by 2–3-fold. Reduced killing velocity, apoptotic blebbing, activation of caspase 3/7 and formation of apoptotic DNA fragments proved that the active and cancer selective peptides, e.g. R-DIM-P-LF11-322, trigger apoptosis, whereas highly active, though non-selective peptides, such as DIM-LF11-318 and RW-AH seem to kill rapidly via necrosis inducing membrane lyses. Structural studies revealed specific toxicity on cancer cells by peptide derivatives with loop structures, whereas non-specific peptides comprised α-helical structures without loop. Model studies with the cancer membrane mimic phosphatidylserine (PS) gave strong evidence that PS only exposed by cancer cells is an important target for specific hLFcin derivatives. Other negatively charged membrane exposed molecules as sialic acid, heparan and chondroitin sulfate were shown to have minor impact on peptide activity.

1. Introduction

Cancer is still a leading cause of death worldwide. In the year 2012, more than 14.1 million people all over the world were diagnosed with cancer (http://globocan.iarc.fr/Pages/fact_sheets_cancer.aspx) resulting in 8.2 million deaths. Since the 1940s and the development of the first chemotherapeutics [1], much progress has been made regarding cancer treatment using chemotherapy, surgery, radiation, targeted therapy and combinations thereof. Still, cancer is not curative in/for many cases and therapy is usually accompanied by severe side effects due to non-specificity for tumor cells. Besides, resistance, formation of metastases leads to poor treatability and bad prognosis as amongst others described for malignant melanoma or glioblastoma, cancers to skin or brain. Hence, many cancer types including malignant melanoma [2,3] show only weak sensitivity to chemotherapy. New approaches of molecular targeted therapy and immunotherapies, as the 2011 FDA approved Ipilimumab only yield a 12.7 months median survival either [4]. Glioblastoma is the most prevalent primary brain tumor and prognosis for this grade IV tumor implicates a 2-year-survival rate of only 5% [5] despite intensive research. Applied therapies like radical surgery, radiotherapy or chemotherapy with the alkylating agent Temozolomide only prolong median survival to 15 months after diagnosis [6].

In search of novel anticancer agents host defense peptides and derivatives thereof have emerged as potential alternative anticancer therapeutics offering many advantages over other therapies [7]. Host

☆ Investigations were supported by the Austrian Science Fund (FWF; grant no. P24608-B23).

* Corresponding authors at: Institute of Molecular Biosciences, Biophysics Division, University of Graz, Humboldtstraße 50/III, A-8010 Graz, Austria.
E-mail addresses: sabrina.riedl@uni-graz.at (S. Riedl), dagmar.zweytick@uni-graz.at (D. Zweytick).

http://dx.doi.org/10.1016/j.bbamem.2015.07.018

defense peptides which are part of the innate immune system of diverse species (e.g. mammals, insects, and amphibians) are mostly cationic but amphipathic, targeting the cell membrane by electrostatic interactions with anionic molecules at the cell surface. Because of their mode of action and specificity — the cell membrane being the major target — resistance and cytotoxicity is less likely to occur [8–10] and thus, in addition they are expected to cause fewer side effects.

Regarding the mode of action of the specific killing by anticancer peptides two general mechanisms, triggering necrosis or apoptosis by anticancer peptides as a consequence of their membrane related mode of killing, have been discussed [10–12]. Both killing, based on necrosis via cell membrane lyses and apoptosis via the mitochondrial lytic effect, seem to be dependent on the presence of anionic lipids. The negatively charged phospholipid phosphatidylserine (PS) located in the outer leaflet of cancer cell plasma membranes can represent such a specific target [13], as cardiolipin, a major anionic phospholipid of the mitochondrial membrane. Other negatively charged molecules, which are also exposed on cancer plasma membranes such as sialic acid, heparin and chondroitin sulfate may play a minor role as peptide targets, since present on neoplastic and non-neoplastic cells, though to different extent [7]. Contrariwise these negatively charged molecules might even be able to protect cells from the interaction with cationic peptides by binding and limiting the access to the plasma membrane [14].

As mentioned above a specific target is provided by cancer cells in the form of the negatively charged phosphatidylserine (PS) which is exposed on the outer leaflet of the cancer cell membrane during malignant transformation [15–20]. In non-cancerous cells the cell surface comprises an overall neutral charge due to their main components: the zwitterionic phosphatidylcholine (PC) and sphingomyelin (SM). Phosphatidylserine together with the major part of phosphatidylethanolamine (PE) assembles the inner leaflet of eukaryotic non-cancerous plasma membranes [21]. This lipid asymmetry of the two membrane leaflets is well documented [22,23] and is maintained by an ATP-dependent aminophospholipid translocase [24]. The loss of membrane asymmetry was shown for several cancer types, including metastases, promising to be a general marker of cancer cells and target for therapy by peptides [13,15–18,20,25,26].

In our study, we focused on the human host defense peptide lactoferricin (hLFcin) which is known to exhibit antimicrobial, antiviral, anti-inflammatory and anticancer activities (for a review see [27]). Human lactoferricin comprises amino acid residues 1–45 of the N-terminus of human lactoferrin (hLF). LF11, an 11 amino acid fragment of hLFcin has been optimized regarding its activity against bacterial [28–30] and cancer membranes [31]. Within this study we report about 3 groups of peptides. The groups are derived from the amino acid stretch 21–31 of hLFcin comprising short non-cancer active peptides, longer cancer active and selective di- (retro) peptides and active but non-selective (di-) peptides.

2. Materials and methods

2.1. Peptides

The hLFcin derived peptides LF11-322 (PFWRIRIRR-NH_2, M = 1298.6 g/mol), its di-retro-peptide R-DIM-P-LF11-322 (PFWRIRIRRPRRIRIRWFP-NH_2, M = 2677.4 g/mol), LF11-316 (RWKRINRQWF-NH_2, M = 1488.8 g/mol), its di-retro-peptide R-DIM-LF11-316 (RWKRINRQWFFWQRNIRKWR-NH_2, M = 2960.5 g/mol), LF11-318 (FWQRRIRRWRR-NH_2, M = 1715.0 g/mol), its di-peptide DIM-LF11-318 (FWQRRIRRWRRFWQRRIRRWRR-NH_2, M = 3413.1 g/mol), the di-retro-peptide R-DIM-LF11-337 (PFWRRRIRIRRRRIRIRRRWFP-NH_2, M = 3204.9 g/mol) and the synthetic peptide RW-AH (WWRRWWRRWRRWWRRWWR-NH_2, M = 3098.4 g/mol) were purchased from NeoMPS, Inc. (San Diego, CA, USA). The purities were >97% as determined by RP-HPLC. Human lactoferricin (hLFcin) (amino acid 37–61 of human lactoferrin) (TKCFQWQRNMRKVRGPPVSCIKRDS), with disulfide bond between Cys_3 and Cys_{20} was purchased from AnaSpec, Inc. (Fremont, CA, USA). Peptides were dissolved in Acetic acid (0.1%, v/v) at concentrations of 3 mg/ml. Peptide solutions were stored at 4 °C and concentrations were determined by measurement of UV-absorbance of tryptophan at 280 nm.

2.2. Cell lines and cultures

Melanoma cell lines from primary (SBcl-2) and metastatic (WM164) lesions were maintained in RPMI 1640 medium with GlutaMAX™ (Gibco®, Life Technologies, USA), supplemented with 2% FBS (fetal bovine serum; Gibco®). Rhabdomyosarcoma cell line (TE671) purchased from ECAAC (Health Protection Agency Culture Collections Salisbury, UK) is cultured in Dulbecco's Modified Eagle Medium with GlutaMAX™ (DMEM, Gibco®, Life Technologies, USA) with addition of 10% FBS (Gibco®). The melanoma cell line A375 purchased from ATCC (American Type Culture Collection, Manassas, Virginia, USA) the glioblastoma cell line U-87mg purchased from CSL (Cell Line Service, Eppelheim, Germany) were cultured in Dulbecco's Modified Eagle Medium with GlutaMAX™ (DMEM, Gibco®, Life Technologies, USA) with addition of 10% FBS (Gibco®) and Minimum Essential Media with GlutaMAX™ (MEM Gibco®) supplemented with 10% FBS (Gibco®), 0.1 mM non-essential amino acids (NEAA; Gibco®) and 1.0 mM sodium pyruvate (Gibco®), respectively. Human melanocytes used as healthy control cells were isolated from foreskin as previously described [31]. Melanocytes were cultured in melanocytes growth medium (PromoCell GmbH, Heidelberg, Germany). Normal human dermal fibroblasts purchased from PromoCell GmbH were cultured in fibroblast growth medium 2 (PromoCell GmbH). All cells were kept in a 5% CO_2 atmosphere at 37 °C. At 90% confluence cells were passaged with accutase (Gibco®, Life Technologies, USA). All cell cultures were periodically checked for mycoplasma.

2.3. Spectroscopy in vitro

Toxicity studies on cells were performed using Glomax Multi + detection system (Promega, Madison, WI, USA).

2.3.1. PI-uptake assay

Cells were collected, resuspended in media and diluted to a concentration of 10^6 cells/ml. Aliquots of 10^5 cells were incubated with peptides for up to 8 h at 37 °C and 5% CO_2. For the measurement of the influence of Ca^{2+} on peptide induced PI-uptake Ca^{2+} was present in the respective media at the following concentrations: 0.4 M (standard level in RPMI 1640 medium), 2.0 M, 5.0 M, 10.0 M and 20.0 M. PI was added and cells were again incubated for 5 min at room temperature in the dark. Excitation and emission wavelengths were 536 nm and 617 nm, respectively. For every experiment with every cell line and every peptide the 0% value (0 μM peptide) and 100% value (addition of Triton X-100) was analyzed. Each experiment was repeated 7 times and medium cytotoxicity was calculated as described previously [31].

2.3.2. Cleavage of sialic acid

To remove sialic acid moieties from the cell surface [32,33], the cells were incubated for 45 min at 37 °C in PBS buffer with 0.1 U/ml neuraminidase from *Clostridium perfringens* purchased from Sigma-Aldrich (Deisenhofen, Germany). The cells were washed twice with buffer, resuspended in media and then incubated with peptides, PI-uptake was determined subsequently as in the absence of sialic acid cleavage (see PI-uptake assay).

2.3.3. Addition of exogenous heparin and chondroitin sulfate

Cells were incubated with 20 μM peptides in the presence and absence (control) of 1 μg/ml and 10 μg/ml heparin (Sigma-Aldrich, Deisenhofen, Germany) or chondroitin sulfate (Sigma-Aldrich,

Deisenhofen, Germany) for 8 h. PI-uptake was determined subsequently as in the absence of heparin or CS (see PI-uptake assay).

2.3.4. MTS viability assay

Cell proliferation was measured by using CellTiter 96® Aqueous One Solution Cell Proliferation assay (Promega). Cells were plated in 96-well plates and grown until confluence in respective medium containing 2% serum at maximum to avoid interference with the MTS compound. Peptides were added to a final concentration of 5–100 μM. After incubation for 24 h at 37 °C (5% CO_2) MTS [3-(4,5-dimethylthiazol-2yl)-5-(3-carboxymethoxyphenyl)-2-(4-sulfophenyl)-2H-tetrazolium]-phenozine methosulfate solution (20 μl/well) was added and cells were again incubated for 2 h at 37 °C (5% CO_2). The MTS compound is bioreduced by cells into a colored formazan product that is soluble in tissue culture medium. The quantity of the formazan product as measured by the amount of 490 nm absorbance is directly proportional to the number of living cells in culture. Data are calculated as a percentage of the control (untreated) samples and represent the average of three wells in one experiment which was repeated three times per cell line.

2.3.5. Caspase-3/7 assay/LDH release assay

Peptide induced caspase-3/7 activity in the melanoma cell lines SBcl-2 and A375 and the glioblastoma cell line U-87mg was determined using the Caspase-Glo® 3/7 Assay (Promega). $2 * 10^5$ cells/ml were seeded in white 96-well plates with clear bottom and grown for 48 h at 37 °C (5% CO_2). Peptides were added to different concentration for 2–4 h. Caspase solution was added to a final 1:1 ratio for 30 min at 37 °C. Luminescence intensity was recorded using Glomax Multi + detection system (Promega). Caspase-3/7 activity was calculated as a multiple of untreated cells.

To determine the amount of nonviable cells the CytoTox-ONE™ Homogeneous Membrane Integrity Assay (Promega), which monitors LDH release (lactate dehydrogenase), was used following the standard protocol. The CytoTox-ONE™ reagent was added to a final 1:1 ratio for 10 min at room temperature. The reaction was stopped by adding the stop solution. Fluorescence intensity was recorded at 590 nm (excitation 560 nm) using Glomax Multi + detection system (Promega). Percentage of LDH release was calculated as described for PI toxicity. Data were calculated as an average of at least three experiments.

2.4. Fluorescence microscopy

Experiments were performed on a Leica DMI6000 B with IMC in connection with a Leica DFC360 FX camera and AF 6000 software (Leica Microsystems, Vienna, Austria).

2.4.1. PI-uptake

Cells ($1–5 \times 10^4$) were seeded on Ibidi μ-Slide 8 wells and grown in 300 μl media for 2–3 days to a confluent layer. Propidium iodide (PI, 2 μl of 50 μg/ml in PBS, Biosource, Camarillo, CA, USA) was added to the well and cell status was checked after 5 min of incubation in the dark at room temperature. Then, peptides were added to the desired concentration and peptide effect was followed immediately. Pictures were taken every 5 or 15 min for up to 8 h from the same section of cells. Excitation and emission wavelength were as follows: PI excitation, 535 nm and emission, 617 nm.

2.4.2. TUNEL staining (in situ direct DNA fragmentation)

DNA fragmentation was detected using In situ Direct DNA Fragmentation (TUNEL) Assay Kit (Abcam, Cambridge, GB). Cells (5×10^4) were seeded on Ibidi μ-Slide 8 wells and grown in 300 μl media for one day to a confluent layer. Peptides were added to the desired concentration and incubated for 2–4 h at 37 °C and 5% CO_2. Cells were then fixed using 1% (w/v) paraformaldehyde in PBS and kept in 70% (v/v) ethanol at −20 °C until use. Cells were stained according to the assay protocol. DNA fragmentation was monitored by fluorescence microscopy. Apoptotic cells show green staining through FITC-labeling (Ex 495 nm, Em 519 nm). Additionally, PI counterstaining was used.

2.5. Circular dichroism spectroscopy

Measurements were performed on a Jasco J 715 Spectropolarimeter (Jasco, Gross-Umstadt, Germany) at room temperature using quartz cuvettes with an optical path length of 0.02 cm. The CD spectra were measured between 260 nm and 180 nm with a 0.2 nm step resolution. To improve accuracy 5 scans were averaged. Peptides were dissolved in 10 mM Hepes (pH 7.4) to a final concentration of 100 μM. Spectra were measured in the absence and presence of 1 mM sodium dodecyl sulfate (SDS) and 1 mM dodecylphosphocholine (DPC) (Avanti Polar Lipids, Alabaster, USA) mimicking cancer and healthy mammalian membranes, respectively. The respective peptide to surfactant molar ratios were 1:25 and 1:100. Background signals were abstracted after measurements [31]. Percentage secondary structure calculations were done using Dichroweb, CDSSTR Convolution Program using reference set 7 [34–36].

2.6. Spectroscopy with model membranes

Leakage and Trp quenching experiments with vesicles were performed using a SPEX Fluoro Max-3 spectrofluorimeter (Jobin-Yvon, Longjumeaum, France) and spectra were analyzed with Datamax software.

2.6.1. ANTS/DPX leakage

Leakage of aqueous contents from liposomes composed of POPS (1-palmitoyl-2-oleoyl-*sn*-glycero-3-phospho-L-serine) or POPC (1-palmitoyl-2-oleoyl-*sn*-glycero-3-phosphocholine) was determined using the 8-aminonaphthalene-1,3,6-trisulfonic acid/p-xylene-bis-pyridinium bromide (ANTS/DPX) assay. Lipid films were prepared, hydrated, measured and analyzed, as described previously [31,37,38].

2.6.2. Trp quenching by acrylamide carrying vesicles

Acrylamide carrying POPC liposomes and pure POPC liposomes were prepared following the protocol for ANTS/DPX containing vesicles described previously [31,37,38] with the exception of the hydration buffer. POPC lipid (20 mg) films for acrylamide carrying liposomes were hydrated with 1 ml 10 mM HEPES (4-(2-hydroxyethyl)-1-piperazineethanesulfonic acid), 68 mM NaCl, 0,4 M acrylamide, pH 7.4, following a standard protocol by incubation at 30 °C with intermediate vigorous vortexing for 1 min every 15 min for 2 h. Following the same protocol pure POPC liposomes were prepared by hydration of POPC lipid films in buffer 10 mM HEPES (4-(2-hydroxyethyl)-1-piperazineethanesulfonic acid), 68 mM NaCl, at pH 7.4 without acrylamide.

Subsequently, the dispersions were extruded 20 times through a polycarbonate filter (Millipore — Isopore™) of 0.1 μm pore size to obtain LUVs. Unilamellarity and size were tested by X-ray and dynamic light scattering, respectively. The acrylamide encapsulating vesicles were separated from free acrylamide by exclusion chromatography using a column filled with Sephadex™ G-75 (Amesham Biosciences, GE Healthcare, Glattbrugg, Switzerland) fine gel swollen in an isosmotic buffer (10 mM HEPES, 140 mM NaCl, pH 7.4). The void volume fractions were collected and the phospholipid concentration was determined by phosphate analysis [37].

The fluorescence measurements were performed in 2 ml of the isosmotic buffer in a quartz cuvette at room temperature. Peptides were diluted with the isosmotic buffer to a final fluorescence intensity of 10^5–10^6. Aliquots of the acrylamide carrying POPC were added to a final peptide to lipid ratio of 1:25 and incubated for 30 min. Tryptophan fluorescence spectra were obtained at room temperature using an excitation wavelength of 282 nm and a slit width of 5 nm for excitation and emission monochromators before and after addition of lipid.

2.7. Differential scanning calorimetry (DSC)

For preparation of liposomes 1 mg of respective phospholipid stock solution was dried under a stream of nitrogen and stored in vacuum overnight to completely remove organic solvents. The dry lipid film was then dispersed in phosphate buffered saline (PBS, 20 mM NaPi, 130 mM NaCl, pH 7.4) and hydrated at a temperature well above the gel to fluid phase transition of the respective phospholipid under intermittent vigorous vortex-mixing. The lipid concentration was 0.1 wt.% for calorimetric experiments. Hydration was carried out in the presence or absence of peptides at a lipid-to-peptide ratio of 25:1 using a protocol described for 1,2-dipamitoyl-sn-glycero-3-phospho-L-serine (DPPS) [39]. Briefly hydration of DPPS films was performed at 65 °C for 2 h with vortexing for 1 min every 15 min. DPPC liposomes were hydrated at 50 °C with vortexing every 15 min for 2 h. The fully hydrated samples were stored for at least 1 h at room temperature until measurement. DSC experiments were performed with a differential scanning calorimeter (VP-DSC) from MicroCal, Inc. (Northhampton, MA, USA). Heating scans were performed at a scan rate of 30 °C/h (pre-scan thermostating 30 min) with a final temperature of approximately 10 °C above the main transition temperature (Tm) and cooling scans at the same scan rate (pre-scan thermostating 1 min) with a final temperature approximately 20 °C below T_m. The heating/cooling cycle was performed three times. Enthalpies were calculated by integration of the peak areas after normalization to phospholipid concentration and baseline adjustment using the MicroCal Origin software (VP-DSC version).

2.8. Zeta potential

Zeta potentials were determined with a Zetasizer Nano ZSP (Malvern Instruments, Herrenberg, Germany) by determining the electrophoretic mobility and applying the Henry equation. The zeta potential was calculated according to the Smoluchovski model used for aqueous solutions. Cells were detached freshly before measurement by addition of accutase. Approx. $5 * 10^4$ cells were suspended in 1 ml 10 mM Hepes, 2 mM CsCl, pH 7.4. If added, peptide or Ca^{2+} concentration was 1 μM, respectively. Three measurements were performed after 5 min of incubation at 37 °C in Cell DTS1070 disposable folded capillary cells (Malvern) with 10–100 runs and 60 s delay between measurements. Attenuation and voltage selection was automatic, analysis was auto-mode.

3. Results

Recently we demonstrated that human lactoferricin derivatives are highly active against cancer cell mimetics as well as against melanoma cells in vitro [31]. In this study we report on the different modes of action of hLFcin derivatives against cancer and non-cancer cells. The eight studied peptides (Table 1) can be divided in three groups. The first group is derived from the amino acid stretch 21–31 of hLFcin, termed LF11 [28,29,31], comprising peptides LF11-316, LF11-318 and LF11-322, which are 9–11 amino acids long. These peptides have already been reported to exert antibacterial activity [30,40], but are within this study tested for antitumor activity. The second group comprises di-peptides that are derived from the first group, such as (retro) repeat derivative with a P(roline) linker, R(etro)-DIM-P-LF11-322 [31] or (retro) repeat derivative without a P(roline) linker, R-DIM-LF11-316. The third group consists of di-peptides derived of LF11, such as the repeat derivative DIM-LF11-318, the (retro) repeat derivative, R-DIM-LF11-337 and the non-LF11 derived synthetic non-di-peptide consisting of only alternating arginines (R) and tryptophans (W), RW-AH (Amphipathic Helix), as a mimic of an ideal membrane active peptide. The peptides of the different groups are in the following described to differ in length, structure, activity and selectivity for cancer cells, targets and killing modes.

Table 1
Overview of peptide sequences, net charge and positive charges of hLFcin derivatives.

Peptide	Sequence	Group	Length [aa]/net charge/no. of R
LF11-322	PFWRIRIRR-NH_2	1	9/+5/4R
R-DIM-P-LF11-322	PFWRIRIRR-P-RRIRIRWFP-NH_2	2	19/+9/8R
LF11-318	FWQRRIRRWRR-NH_2	1	11/+7/6R
DIM-LF11-318	FWQRRIRRWRR-FWQRRIRRWRR-NH_2	3	22/+13/12R
LF11-316	RWKRINRQWF-NH_2	1	10/+5/3R
R-DIM-LF11-316	RWKRINRQWF-FWQRNIRKWR-NH_2	2	20/+9/6R
R-DIM-LF11-337	PFWRRRIRIRR-RRIRIRRRWFP-NH_2	3	22/+13/12R
RW-AH	WWRRWWRRWRRWWRRWWR-NH_2	3	18/+10/9R

Aa, amino acid; no., number.

3.1. Toxicity and mechanistic studies

3.1.1. Membrane disintegration and time dependence — PI-uptake-cell death

Cytotoxic activity of the peptides towards melanoma cells of primary (SBcl-2) and metastatic lesions (WM164), a melanoma cell line (A375), a rhabdomyosarcoma cell line (TE671), a glioblastoma cell line (U-87mg) and their healthy counterparts differentiated non-tumorigenic melanocytes and normal human dermal fibroblasts (NHDF) was determined by measurement of PI-uptake, which is an indication for the loss of cell membrane integrity and cell death (Fig. 1, Table 2). Cells were incubated in respective media containing serum for up to 8 h in the presence of peptides at 20 μM peptide concentration.

Short peptides LF11-322, LF11-316 and LF11-318, reported to be active against *Escherichia coli* and bacterial lipid model systems [28,30,40] were shown in this study and previously (LF11-322) [31] to exert only negligible antitumor activity against the different tested cancer types (<30%, see Fig. 1). The (retro) di-peptides R-DIM-P-LF11-322, R-DIM-LF11-316 and DIM-LF11-318, as well as the synthetic peptide RW-AH however exhibited highly increased activity against all human cancer cell lines (80–100% after 8 h of incubation) with no preference of a certain cancer type, though with different velocity. Accordingly Fig. 1 shows that the cancer active di-peptides (second group) R-DIM-P-LF11-322 and R-DIM-LF11-316 do not reach 50% killing of cancer cells before 2–4 h of incubation. Contrary the di-peptides of the third group DIM-LF11-318 and RW-AH reach 50% killing up to 1 h of peptide incubation, however against all cell types, cancer as well as non-cancer cells, indicating fast killing and no selectivity only for cancer cells.

The non-active short peptides LF11-322, -316 and -318 and the slowly but highly cancer active peptides of the second group R-DIM-P-LF11-322 and R-DIM-LF11-316 however were not shown to be toxic for non-cancer cells as melanocytes and normal human dermal fibroblasts (NHDF). Fig. 1 reveals high specificity of the peptides of the second group for cancer cells of up to 13-fold for R-DIM-P-LF11-322 (SBcl-2 over melanocytes) and 4.5-fold for R-DIM-LF11-316 (A375 over NHDF) (see $LC_{50\ PI}$, Table 2).

Correlation of slow killing with specificity was also confirmed by live microscopic inspection of the melanoma cell line SBcl-2 (data not shown) revealing different killing velocity of the specific peptide R-DIM-P-LF11-322 and the non-specific peptide DIM-LF11-318. Only minor membrane damage (PI-uptake) of SBcl-2 and no damage of NHDF by R-DIM-P-LF11-322 were observed after 1 h, whereas the non-specific peptide DIM-LF11-318 had already killed all cells of SBcl-2 and NHDF in the same time. This is comparable to cell toxicity on SBcl-2 by R-DIM-P-LF11-322 after 8 h of incubation. R-DIM-P-LF11-322 did not cause cell damage of NHDF after 8 h.

3.1.2. MTS — cell viability

To determine long-term toxicity of peptides on melanoma or melanocytes (or dermal fibroblasts), a MTS cell proliferation assay was used to elucidate cell viability upon 24 h after incubation with variant peptide concentrations ($LC_{50\ MTS}$, Table 2). As shown, LF11-322 affects

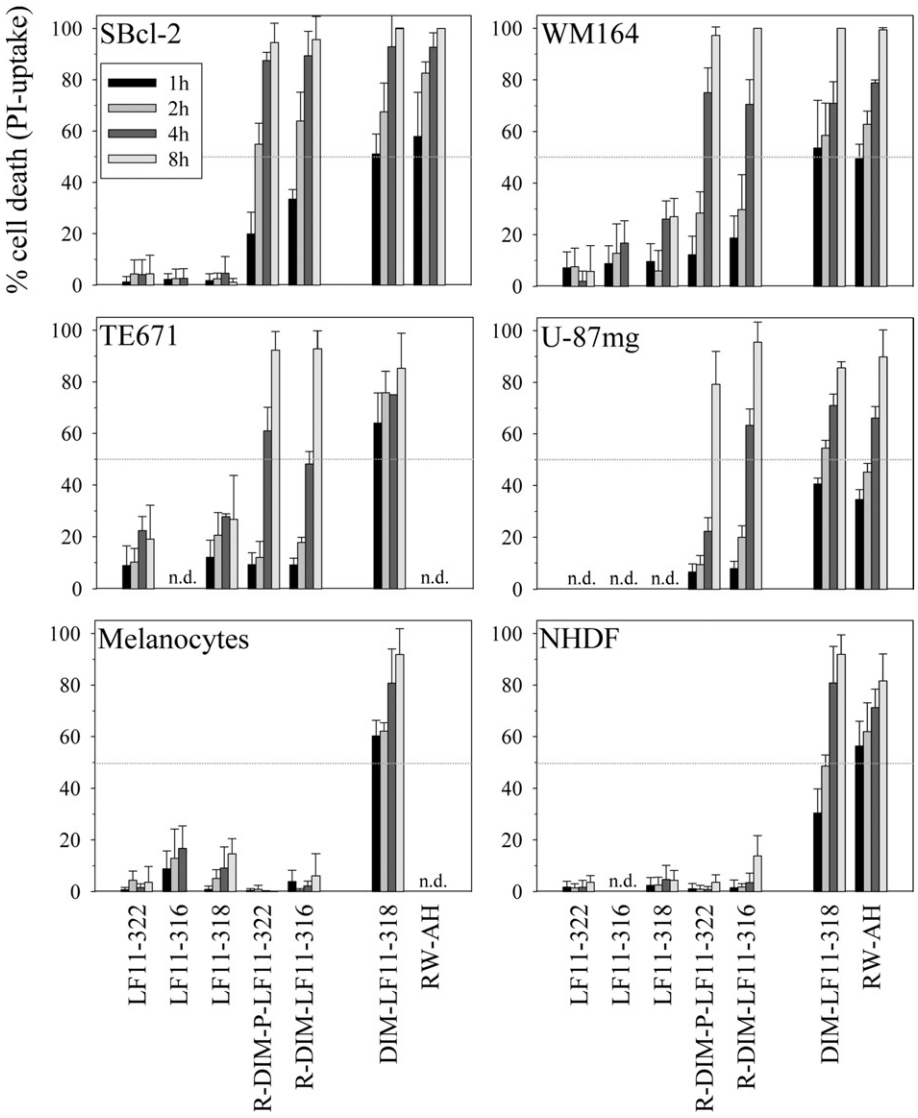

Fig. 1. PI-uptake of various cancerous and non-cancerous cell lines upon incubation with 20 μM peptide: Time dependent (1–8 h) cytotoxic activity of LF11-322, LF11-316, LF11-318, R-DIM-P-LF11-322, R-DIM-LF11-316, DIM-LF11-318 and RW-AH against primary lesions of non-tumorigenic melanoma (skin cancer) cell line SBcl-2, melanoma metastases WM164, differentiated control cells of primary cultures of melanocytes of foreskin, rhabdomyosarcoma (soft tissue cancer) cell line TE671, glioblastoma (brain cancer) cell line U-87mg and normal human dermal fibroblast cell line NHDF at 20 μM peptide concentration is shown; n.d. not determined.

Table 2
Comparison of LC_{50} values [μM] of treated melanoma, melanocytes and fibroblasts determined through PI-uptake (8 h) and MTS cell viability assay (24 h).

Peptide	Melanoma A375 (*SBcl-2)		Dermal fibroblasts NHDF (*Melanocytes)	
	$LC_{50\ PI}$ [μM]	$LC_{50\ MTS}$ [μM]	$LC_{50\ PI}$ [μM]	$LC_{50\ MTS}$ [μM]
LF11-322	(*>80)	(*>100)	(*>80)	>100
R-DIM-P-LF11-322	9.5 ± 0.3 (*5.9 ± 0.3)	23.3 ± 1.7 (*10.4 ± 0.7)	65.1 ± 2.5 (*>80)	65.1 ± 0.3
R-DIM-LF11-316	6.5 ± 0.4	21.0 ± 1.2 (*16.0 ± 0.5)	33.2 ± 0.7	61.8 ± 0.1
R-DIM-LF11-337	3.5 ± 0.4	12.3 ± 1.3 (*5.0 ± 0.4)	11.7 ± 3.2	22.8 ± 0.1
DIM-LF11-318	3.8 ± 0.5	9.3 ± 0.8 (*9.4 ± 0.5)	2.2 ± 0.9 (*14.0 ± 0.6)	13.9 ± 0.4
RW-AH	4.5 ± 0.02	8.4 ± 0.5 (*4.6 ± 0.2)	10.0 ± 0.4	9.6 ± 0.2

Data for PI measurements from at least seven and for MTS from at least three experiments are presented as mean ± SD.

cancer cells only marginally ($LC_{50\ SBcl\text{-}2\ and\ NHDF}$ > 100 μM; Table 2). R-DIM-P-LF11-322 and R-DIM-LF11-316 exhibit highly increased cancer toxicity evidenced by $LC_{50\ SBcl\text{-}2}$ of 10 μM or 16 μM, respectively (Table 2), whereas viability of fibroblasts NHDF is less reduced with 6.5-fold or 3.9-fold specificity for cancer cells exerted by the respective peptides. DIM-LF11-318, DIM-LF11-337 and RW-AH also show high activity against cancer cells, however as well against non-cancer cells confirming their low selectivity demonstrated by the PI uptake studies shown in Fig. 1 (Table 2) with only 1–2 fold selectivity for cancer cells.

3.1.3. Morphology of dying cells, caspase-3/7 activity and TUNEL assay — apoptosis or necrosis

As observed in the PI-uptake studies (Fig. 1) the selective peptides R-DIM-P-LF11-322 and R-DIM-LF11-316 were killing cancer cells more slowly compared to the non-specific peptides DIM-LF11-318 and RW-AH. Delayed cell death can be a hint for killing via apoptosis. This notion was confirmed by the observation of shrinking and apoptotic like blebbing of rhabdomyosarcoma cells (TE671) and melanoma cells

(SBcl-2) before death (PI-uptake) that was observed during incubation of the cells with the specific peptide R-DIM-P-LF11-322 (Fig. 2A1 and A2, arrows indicate appearance of blebs upon incubation with peptide).

The non-specific peptide DIM-LF11-318 induced a fast killing and slight swelling of the melanoma cells (SBcl-2) with visible lyses of the membrane during the PI-uptake (Fig. 2A3), being characteristic for uncontrolled killing via necrosis.

Further evidence is given by results obtained for caspase-3/7 activity. Melanoma cells are known to block apoptosis by inhibiting the activation of caspase-3 and -7 [13,41]. As illustrated in Fig. 2B (upper bar diagram) the slowly killing peptide, R-DIM-P-LF11-322 (black bars), which had shown induced apoptotic membrane blebbing, clearly displayed increased caspase-3/7 activity of SBcl-2 (2–3-fold of control) after 4 h of incubation with the peptide at concentrations of

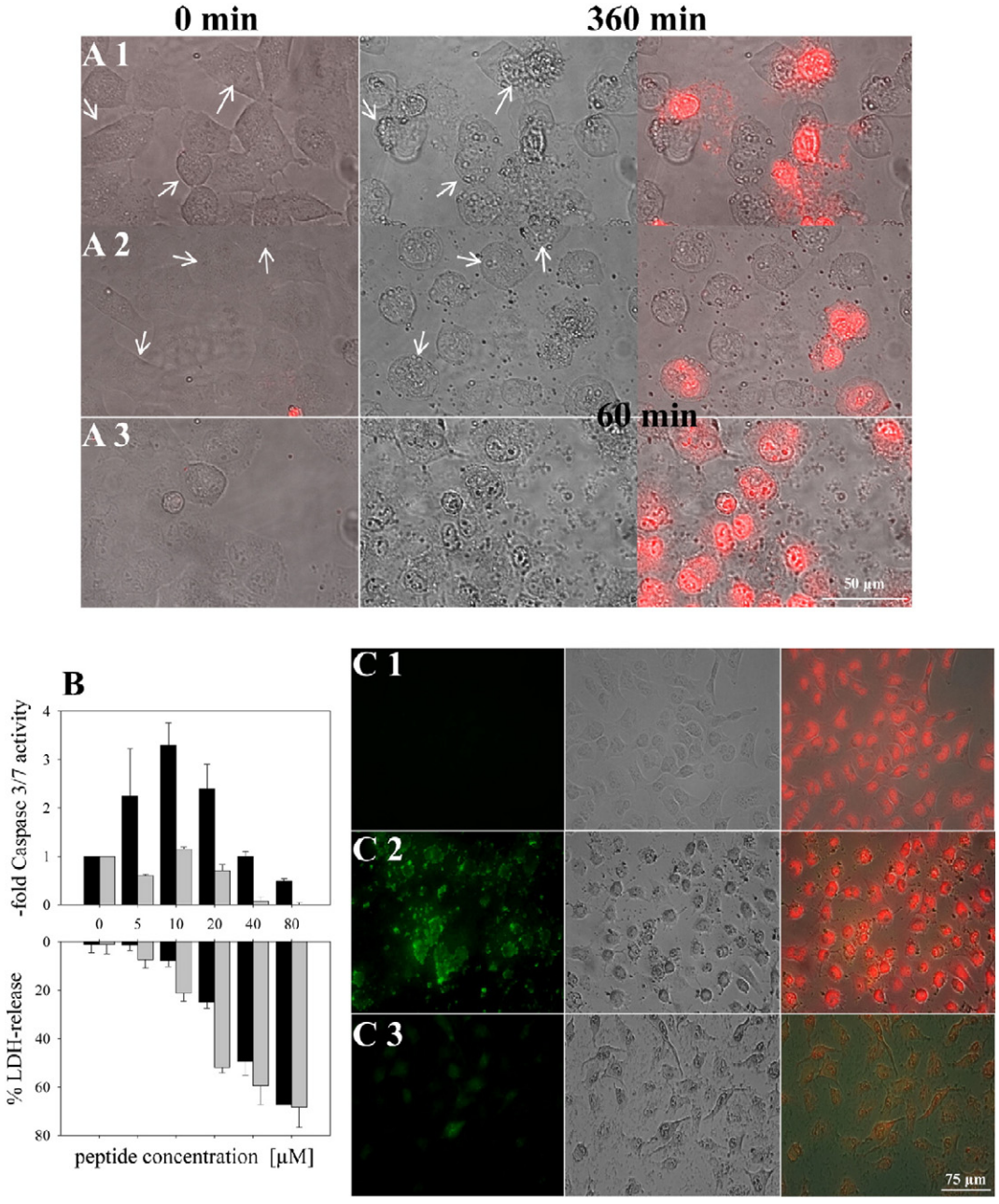

Fig. 2. A: PI-uptake of cancer cells indicating different killing mechanisms by the specific peptide R-DIM-LF11-322 (A1: TE716, A2: SBcl-2) and the non-selective peptide DIM-LF11-318 (A3: SBcl-2). Overlay of fluorescence micrographs and bright field are shown at the left (0 min peptide incubation) and the right side; A1: 360 min peptide incubation, A2 and A3: 60 min peptide incubation. The respective bright field pictures with peptide incubation are shown in the middle. Signs of killing via apoptosis by appearance of blebs (middle, arrows) and shrinking of rhabdomyosarcoma cells (TE671) (A1) after 360 min of incubation and melanoma cells (SBcl-2) (A2) after 60 min of incubation with 20 µM R-DIM-LF11-322 are shown in bright field (middle). Signs of necrosis by faster killing (1 h), swelling and membrane lyses of SBcl-2 melanoma cell line after 1 h of incubation with 20 µM DIM-LF11-318 (A3) bright field (middle) and overlay with fluorescence (right) are shown. B: Fold caspase-3/7 activity (top) of melanoma cell line SBcl-2 after 4 h of incubation indicating induction of apoptosis by the peptide R-DIM-P-LF11-322 (black bars) and % LDH-release (bottom) upon 2 h of incubation with peptides R-DIM-P-LF11-322 (black bars) and DIM-LF11-318 (gray bars) at different peptide concentrations indicating cell damage and killing via necrosis by DIM-LF11-318. C: DNA fragmentation of melanoma cell line SBcl-2 upon 2 h of incubation without peptide (C1), with 10 µM R-DIM-P-LF11-322 (C2) and with 10 µM DIM-LF11-318 (C3). On the left side FITC-labeled DNA-fragments (green) are shown indicating apoptosis upon incubation with R-DIM-P-LF11-322 (C2). In the middle bright field pictures indicate membrane disintegration in the presence of R-DIM-P-LF11-322 (C2) and DIM-LF11-318 (C3). On the right side overlay pictures of BF, PI-fluorescence (red) and FITC-labeled DNA-fragments are shown.

5–20 μM. The fast killing derivative DIM-LF11-318 (gray bars) did not show any increased levels of caspase-3/7 activity at any concentration, suggesting other killing mechanism than apoptosis. In combination with the simultaneous measurement of the release of LDH (lactate dehydrogenase), a soluble cytosolic enzyme that is released into the culture medium, loss of membrane integrity resulting from either apoptosis or necrosis can be evidenced (Fig. 2B, lower bar diagram). In the case of the peptide DIM-LF11-318 a strongly increased LDH-release was observed, indicative of severe membrane disintegration, already in the presence of low concentrations of the peptide (gray bars), suggesting necrosis to be induced by this peptide. As can be further seen in Fig. 2B above 40 μM also R-DIM-P-LF11-322 (black bars) induced an increase of LDH-release, whereas no caspase-3/7 activity was observed.

Further supporting results were obtained with a direct in situ DNA fragmentation assay, another possibility to differentiate between necrotic and apoptotic killing. Fig. 2C displays microscopy images of melanoma cell line SBcl-2 in the absence (Fig. 2C1) and presence of peptides R-DIM-P-LF11-322 (Fig. 2C2) and DIM-LF11-318 (Fig. 2C3). On the left side FITC-labeled DNA-fragments (green) are shown indicating potential apoptosis. No green fluorescence signal of the FITC-dUTP labeled DNA fragments is visible without peptide and in the presence of 10 μM DIM-LF11-318 (2 h of incubation) indicating absence of apoptosis. Contrary SBcl-2 cells exposed to specific peptide R-DIM-P-LF11-322 (10 μM, 2 h of incubation) exhibit distinct green fluorescence signals of the FITC-dUTP labeled DNA fragments indicative for apoptosis (Fig. 2C2). In the middle bright field (BF) pictures indicate membrane disintegration only in the presence of R-DIM-P-LF11-322 (Fig. 2C2) and DIM-LF11-318 (Fig. 2C3). On the right side overlay pictures of BF, PI-fluorescence and FITC-labeled DNA-fragments are shown. Red fluorescence occurs in any cases, since the experiment involves fixation of cells, different to the studies described before, where PI-uptake was only peptide induced. In the case of cells incubated with DIM-LF11-318 the red fluorescence is less intense (more diffuse), since membrane lyses upon incubation with this peptide induces degradation and release of DNA fragments.

Selectivity and structural studies—circular dichroism spectroscopy analysis of the peptides LF11-322 and R-DIM-LF11-322 was reported in a recent study [31]. Fig. 3A now compares the CD-structural results of R-DIM-P-LF11-322, R-DIM-LF11-316 and DIM-LF11-318. R-DIM-P-LF11-322 in solution is mainly unstructured and is showing β-sheet conformation and turns to a similar extent [31]. Since CD-experiments in lipidic environment as POPS or POPC deliver rather noisy data, SDS was taken as negatively charged cancer and DPC as neutral non-cancer mimic. In the presence of the cancer mimic SDS and at a peptide-to-lipid ratio of 1:25 R-DIM-P-LF11-322 exhibits a significant increase of β-sheet conformation (30 to 41%). The structure of the peptide in the presence of the healthy mimic DPC is comparable to its structure in solution, indicating a structure dependent cancer selective toxicity of this peptide, which has already been shown previously [31]. Similarly, the cancer-specific peptide R-DIM-LF11-316 only showed a significant change in secondary structure in the presence of the cancer mimic SDS, the α-helical conformation thereby increased from 2% to 22%. In contrast, the non-selective peptide DIM-LF11-318 changes its conformation, though unstructured in solution, massively in the presence of both, the cancer and the non-cancer mimic system. This goes in hand with its non-selective activity. Further it changes its conformation of 6% α-helical to 75% α-helical in the presence of SDS and 72% in the presence of DPC. Also the structure predictions performed by the program PEP-FOLD [42–44] (http://bioserv.rpbs.univ-paris-diderot.fr/PEP-FOLD/) (Fig. 3 colored structures in center) reveal a β-strand conformation for R-DIM-P-LF11-322 with a loop, two α-helices separated by a loop for R-DIM-LF11-316 and α-helix for DIM-LF11-318 without a loop, which is in agreement with CD spectra of the peptides in the presence of model systems. PEP-fold structure predictions for likewise less selective peptide R-DIM-LF11-337 and non-selective peptide RW-AH as well show helical structures without a loop, more extended in case of the latter. The selective mother peptide hLFcin reveals confirmation with a loop between an α-helical and an extended non-structured part, which is in agreement with structural data reported before [27]. Also the selective peptide R-DIM-LF11-316 revealed a conformation with a loop, though in this case breaking two α-helical segments. As can be seen in Fig. 3B the loop structures relate to high cancer specific peptides being toxic for the melanoma cell line A375 and the glioblastoma cell line U-87mg but non-toxic for normal human dermal fibroblasts NHDF, whereas the non-specific peptides exhibit α-helical structures without a loop exhibiting toxicity for all cell types. Fig. 3B also demonstrates the highly increased activity of R-DIM-P-LF11-322 and R-DIM-LF11-316 compared to the activity of their original parent peptide hLFcin of up to 10-fold in A375 and 2–3-fold in U-87mg.

3.2. Potential molecules for peptide interaction

The studied peptides exhibit positive net charges (Table 1), mainly via arginines (and lysines), a potential target thereof are negatively charged cell components on the surface and subsequently in the inside of cells.

As known, cancer cell surfaces differ from that of non-cancer cells by increased exposure of negatively charged PS [7,11], which might represent a specific target for the cationic peptides. Other negative charges exposed are present on cancer and non-cancer cells, as sialic acid, being part of glycoproteins (mucins), partially overexpressed by some cancer types [45–47]. Changes in surface expression of glycosaminoglycans like e.g. heparan or chondroitin sulfate also present on cancer and non-cancer cells are characterized by partially increased or decreased levels on cancer surfaces of different cancer types [7].

3.2.1. Zeta potential of cancer and non-cancer cell surfaces — electrostatic interactions

As demonstrated by measurement of the zeta potential of non-cancer cells NHDF, low tumorigenic melanoma cells from primary lesions SBcl-2 and melanoma cells from metastases WM164 the zeta potential decreases with malignity from quasi neutral for non-malignant NHDF (0 mV) to −25 mV and to −35 mV for SBcl-2 and metastases WM164, respectively (Fig. 4A). The addition of the peptide R-DIM-P-LF11-322 to the cancer cells shifted the zeta-potential significantly (by about 10 mV) to neutral levels, such as the addition of Ca^{2+} ions. This strongly indicates an electrostatic interaction between the positive charges of the peptide and negative charges of the cancer surface. The addition of the peptide DIM-LF11-318 shifts the zeta potential more strongly (by about 20 mV), probably due to hydrophobic additional to the electrostatic interactions. It has to be mentioned, that peptide incubation was limited to 5 min, to avoid membrane lyses that would expose PS, normally on the inside of the cell membrane, overlapping with the changes in zeta potential by binding of peptides to the outside. Addition of Ca^{2+} or peptides R-DIM-P-LF11-322 and DIM-LF11-318 with neutral surface of non-cancer cells NHDF indicate no electrostatic interaction with the surface of the cells due to negligible shifts of the zeta potentials observed.

However as demonstrated in Fig. 4B for longer peptide interaction only the toxicity of the specific peptide R-DIM-P-LF11-322 on melanoma cell line SBcl-2 is significantly affected by the presence of Ca^{2+} ions. For example, after 4 h the PI-uptake of SBcl-2 in the presence of 20 μM R-DIM-P-LF-322 is reduced from 80% at normal level of Ca^{2+} (0.4 mM) to 20% at the highest concentration of Ca^{2+} tested (20 mM) indicating a strong competition of the peptide and Ca^{2+} for a negatively charged target on the cancer membrane. After 8 h however the Ca^{2+}-level does no longer affect the peptide activity, the peptide can either displace the Ca^{2+} or after 8 h Ca^{2+} has already been internalized. Activity of the non-specific peptide DIM-LF11-318 however does not seem to be affected by Ca^{2+}. Only very high Ca^{2+}-levels have an impact

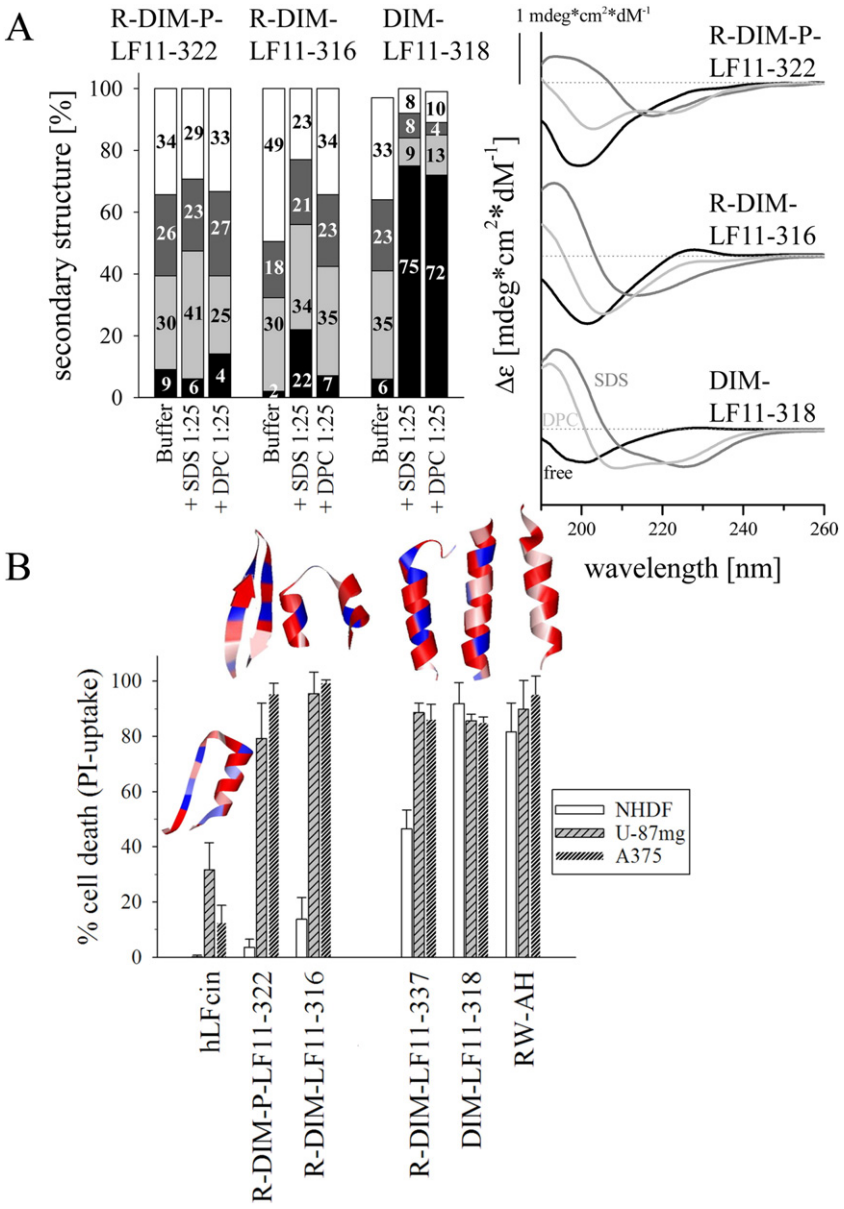

Fig. 3. Correlation of peptide structure and cancer specific cytotoxicity. A: Secondary structures of R-DIM-P-LF11-322 [31], R-DIM-LF11-316 and DIM-LF11-318 in Hepes buffer (black lines) or presence of SDS (gray lines) and DPC (light gray lines) at peptide to surfactant ratios of 1:25 calculated from CD spectra using Dichroweb, CDSSTR Convolution Program [34–36]. The α-helical content is shown in black at the bottom; β-turns are shown in light gray; turns are shown in dark gray; random coil structures are shown in white at the top. Specific peptides R-DIM-P-LF11-322 and R-DIM-LF11-316 change their secondary structure only in the presence of the cancer mimic SDS. The less specific peptide DIM-LF11-318 shows a change in secondary structure in the presence of both, SDS and DPC. B: The bars show cytotoxicity on cell lines of melanoma A375, glioblastoma U-87mg and normal human dermal fibroblasts NHDF upon 8 h of incubation with 20 μM parent peptide hLFcin and cancer specific derivatives R-DIM-P-LF11-322 and R-DIM-LF11-316 and less specific derivatives R-DIM-LF11-337, DIM-LF11-318, as well as synthetic peptide RW-AH. On top PEP-FOLD secondary structure predictions [42,44] of peptides are shown. HLFcin is the only peptide containing a disulfide bridge. R-DIM-PEP-LF11-322 is the only peptide being predicted to form a β-sheet. Positively charged amino acids like Arg are colored in red, more hydrophobic amino acids like Trp, Phe and Ile are colored in pink, violet and blue, respectively. Peptides adopting a predominantly helical (amphipathic) structure exhibit non-selective activities on cancer cells and normal cells, as well. Peptides comprising a β-sheet or a helical structure interrupted by a turn (loop) act more highly specific on cancer cells.

at 1–4 h of incubation, indicating that the non-specific peptide is much less dependent on a negatively charged target on the cell surface than R-DIM-P-LF11-322, which might explain the interaction with cancer and non-cancer cells.

3.2.2. Phosphatidylserine — a negatively charged phospholipid only exposed on the surface of cancer cells

A potent target of anticancer peptides is described to be the negatively charged lipid phosphatidylserine [7,11] specifically exposed by cancer cells [13,15]. Therefore liposomal mimics of human cancerous membranes are applied, as DPPS or POPS to study the peptide cancer membrane interaction. As reported previously the specific peptide R-DIM-P-LF11-322 induces membrane permeabilization of POPS bilayers whereas the non-cancer mimic POPC is not affected [31]. As demonstrated in Fig. 5A ANTS/DPX leakage of liposomes composed of the cancer mimic POPS is, besides by R-DIM-P-LF11-322, only induced by other in vitro active (retro-) di-peptides as R-DIM-LF11-316, R-DIM-LF11-337, DIM-LF11-318 and the synthetic peptide RW-AH. The short parents LF11-322, -316 and -318, which are not active in vitro, in accordance show only minor induction of membrane leakage of POPS. Membrane interaction with PS is also confirmed by differential scanning calorimetry (DSC) (Fig. 5B), where severe membrane perturbation of DPPS was shown by the in vitro active peptides. Upon incubation with the di-peptides and RW-AH the transition temperatures (T_m)

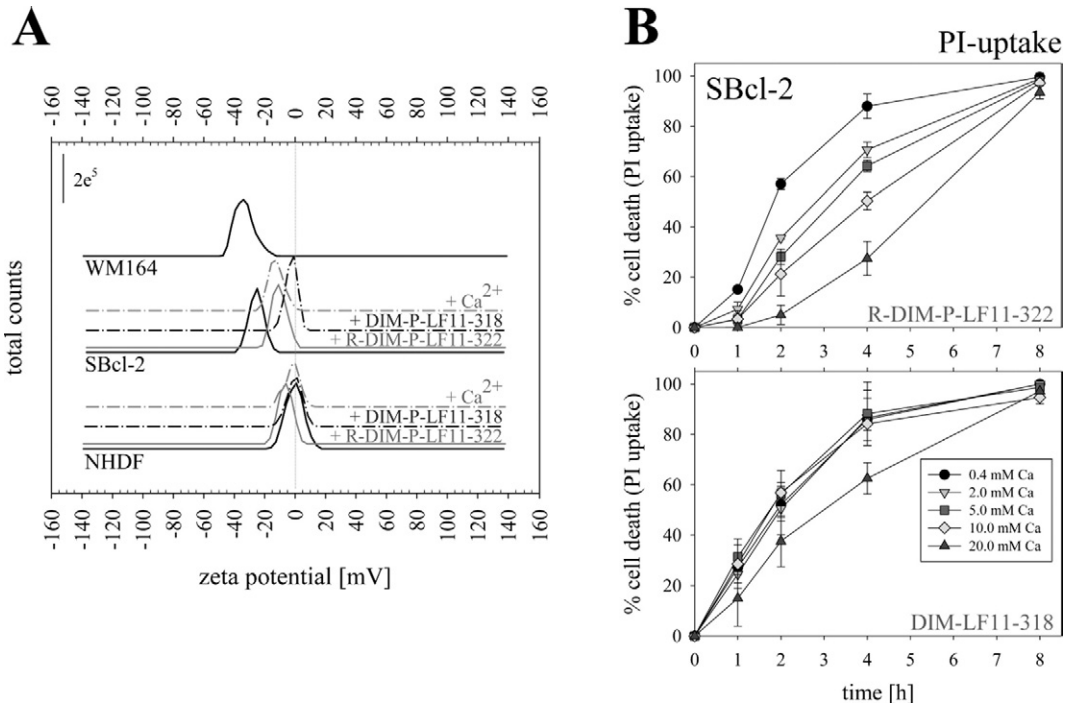

Fig. 4. Cell zeta potential and interaction with positive charges. A: Zeta potential of non-cancer cells NHDF (normal human dermal fibroblasts) compared to melanoma cancer cells of primary lesions SBcl-2 and metastases WM164 in the absence (black lines) and in the presence of 1 μM peptide R-DIM-P-LF11-322 (gray lines), 1 μM DIM-LF11-318 (intermittent black lines) and in the presence of 1 μM Ca (intermittent gray lines) (5 min incubation time). Cancer cells exhibit more highly negative zeta potentials in comparison with normal fibroblasts. Peptides and calcium can compensate the negative zeta potential indicating an interaction of peptides and the negatively charged surface of the cancer cells. The addition of Ca^{2+} or peptides to normal fibroblasts does however not show any interaction on the cell surface. B: Cell death in the presence of peptides affected by increasing amounts of Ca^{2+}. The activity of the specific peptide R-DIM-P-LF11-322 (upper) is affected by increasing amounts of Ca^{2+}, indicating sole interaction with negative charges on the surface of cancer cells. The activity of the non-specific peptide DIM-LF11-318 (lower) is less dependent on a negative cell surface.

of the cancer mimic were shifted to lower temperatures by several degrees. Cooperativity was increased, indicated by an increase of the half-width ($T_{1/2}$). The transitions were mainly split in 2 or more peaks, due to peptide affected lipid domains, where the lower temperature domain is probably more highly enriched in peptide. In some cases also a strong decrease of the phase transition enthalpy (ΔH_{cal}) indicated severe membrane destabilization.

3.2.3. Phosphatidylcholine — a zwitterionic (neutral) phospholipid present on the surface of cancer and non-cancer cells

As shown before, interaction with the omnipresent (cancer and non-cancer) lipid phosphatidylcholine can go in hand with toxicity on cancer and non-cancer cells [31]. ANTS/DPX leakage of liposomes composed of the non-cancer mimic POPC indeed revealed no membrane permeabilization by the cancer specific peptide R-DIM-P-LF11-322 (Fig. 5A). This is in correlation with its non-toxicity on non-cancer membranes. On the other hand strong membrane permeabilization by the non-specific peptide RW-AH (already 70% leakage at 2 μM RW-AH) is in correlation with its toxicity on fibroblasts and melanocytes. This result was also confirmed by DSC, showing no interaction by R-DIM-P-LF11-322, but only perturbation of PC bilayers by RW-AH (Fig. 5B). In the presence of the peptide RW-AH the DPPC liposomes were massively influenced, the phase transition was nearly completely abolished in the temperature range studied. Surprisingly, it could be shown that the non-specific peptide DIM-LF11-318 however, though interacting in vitro with non-cancer membranes, did not cause membrane permeabilization nor membrane perturbation of PC bilayers, such as the non-specific peptide RW-AH. As demonstrated in Fig. 6 DIM-LF11-318 is however able to penetrate POPC bilayers though apparently without causing severe membrane damage (Fig. 5B). Inside the cell, DIM-LF11-318 probably may cause damage by contact with other (inner) membrane components or interact with other negatively charged inner targets (see discussion Fig. 7). This was indicated by a decrease of nearly 50% of the Trp fluorescence of the peptide DIM-LF11-318 in the presence of POPC liposomes containing the quencher acrylamide only inside (Fig. 6) compared to the presence of PC liposomes containing only buffer. This can only be the case if the peptide DIM-LF11-318 penetrates the PC membrane getting access to the quencher. The emission wavelength did not show any blue-shift, confirming no membrane permeabilization. Whereas the specific peptides R-DIM-P-LF11-322 and R-DIM-LF11-316 showed no change in fluorescence intensity in the presence of both vesicle types, containing acrylamide or containing buffer. No blue-shift was revealed indicating no interaction at all with the healthy mimic correlating with its non-interaction with healthy cells. Also in accordance with the demonstrated strong interaction of RW-AH with PC bilayers in Fig. 5 by permeabilization and perturbation Fig. 6 shows entrance of RW-AH into PC bilayers and thereby access to acrylamide and/or release of acrylamide. The induced blue-shift of about 10 nm (Fig. 6) confirms the strong membrane perturbation of PC bilayers (Fig. 5).

3.2.4. Sialic acid — a negatively charged molecule increased on surfaces of cells of some cancer types

Probable interaction with other negatively charged membrane components, as e.g., sialic acid, being part of glycoproteins, which are partially overexpressed by some cancer types [45–47], was studied. Therefore neuraminidase from *C. perfringens* to malignant melanoma cell line A375, melanoma metastases WM164, glioblastoma cell line U-87mg and the rhabdomyosarcoma cell line TE671 to cleave off terminal sialic acid residues which are α-2,3-, α-2,6- or α-2-8-linked to oligosaccharides, glycolipids or glycoproteins was applied (Table 3). However cleavage of sialic acid residues from the cancer types tested did not significantly change activity of the studied peptides up to 8 h of incubation, indicating that sialic acid is neither a main target for the studied peptides nor able to protect the cancer cells from the toxic effect of peptides. Only in the case of U-87mg cells removal of sialic acid

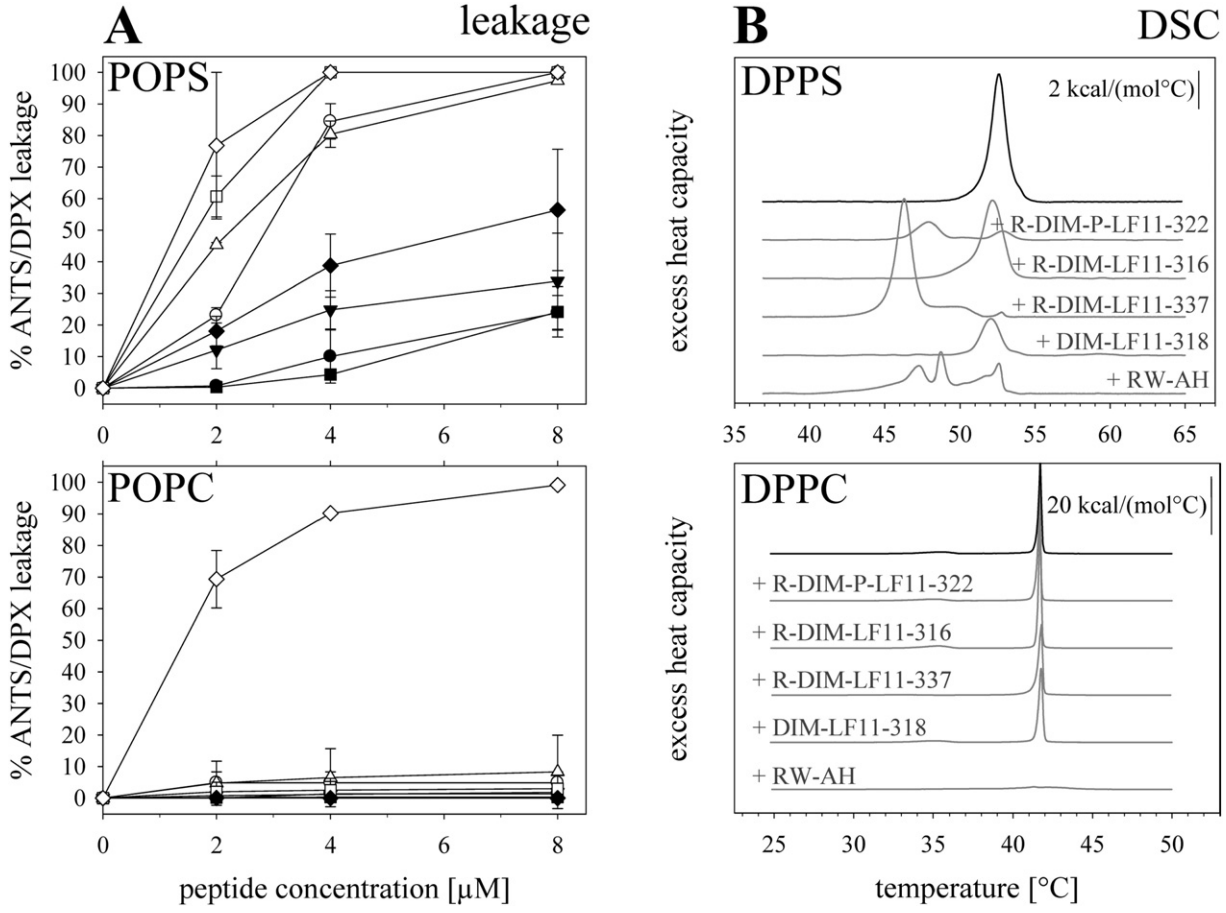

Fig. 5. Interaction of peptides with cancer and non-cancer membrane model systems. A: ANTS/DPX leakage of LUVs composed of cancer mimic POPS (top) or non-cancer mimic POPC (bottom) as a function of concentration of LF11-322 (●), R-DIM-P-LF11-322 (○), LF11-318 (▼), DIM-LF11-318 (△), LF11-316 (■), R-DIM-LF11-316 (□), R-DIM-LF11-337 (♦) and RW-AH (◊). Concentration of LUVs was 50 μM and temperature was kept at 37 °C during measurements. Complete lyses was determined by addition of Triton X-100 and zero levels correspond to fluorescence before peptide addition. B: DSC thermograms of cancer mimic DPPS (top) or non-cancer mimic DPPC (bottom) in the absence (black) and presence of elevated peptides (gray) (25:1, lipid-to-peptide molar ratio). For clarity, the DSC curves were displayed on the ordinate by an arbitrary increment. Peptides active in vitro are active on the model system PS. Only the di-peptides R-DIM-P-LF11-322, R-DIM-LF11-316, R-DIM-LF11-337, DIM-LF11-318 and the synthetic peptide RW-AH show strong interaction with the cancer mimic system PS. Only the synthetic peptide RW-AH shows permeabilization and perturbation of PC membranes.

slightly increased activity of R-DIM-P-LF11-322 and DIM-LF11-318 by approximately 10%. On the surface of these cancer cells sialic acid might slightly shield the cells from the peptide access to the cell membrane.

3.2.5. Heparin and chondroitin sulfate — a negatively charged molecule increased or decreased on surfaces of cancer cells

Other negative charges exposed on the surface of cancer, but also of non-cancer cells are heparan sulfate (HS) and chondroitin sulfate (CS) [7]. Competition with heparin or chondroitin sulfate (CS) was therefore tested by addition of exogenous heparin and CS in concentrations of 1 μg/ml and 10 μg/ml to melanoma cells A375 (Table 4). No significant effect on the di-peptide activity was observed. The activity of the short peptides LF11-322 and LF11-318 was however increased to some extent. Higher amounts of heparin were not used, since at elevated concentrations observed effects could become non-specific because HS might interfere with electrostatic interactions in general [48]. The results indicate neither a potent target nor a protective function by HS and CS on peptide activity.

4. Discussion

Recently it has been shown that hLFcin derivatives can target the negatively charged phospholipid phosphatidylserine [31] which is specifically exposed by cancer cells and metastases [13,15,49]. In this previous study we have demonstrated that an enhanced membrane interaction of the peptide R-DIM-P-LF11-322 (a di-retro-peptide derived from the short membrane active peptide LF11-322) [29,30] with the cancer mimics anionic PS and mixtures of PS and neutral PC correlates with highly increased activity against melanoma cells whereas increasing interaction of N-acyl-LF11-322 with the healthy mimic PC correlated with decreased specificity indicated by intensified interaction with differentiated cells like melanocytes. In the present study we investigated the cytotoxic effects of LF11-322 and R-DIM-P-LF11-322 and other LF11 derivatives like R-DIM-LF11-316 (derived from LF11-316), R-DIM-LF11-337 and DIM-LF11-318 (derived from LF11-318) for cancer cell lines isolated from a primary malignant melanoma, a melanoma metastasis, glioblastoma (brain tumor) and rhabdomyosarcoma (soft tissue tumor) and compared to toxicity on differentiated cells like human melanocytes and human dermal fibroblasts. Further a synthetic peptide RW-AH, comprising an alternating sequence of the amino acids Arg and Trp, constituting an amphipathic α-helix, was probed to determine potential characteristics for α-helical membrane active peptides. Mechanistic studies aimed to identify the different mode of actions (Fig. 7) of active-selective and active-non-selective peptides. For (bovine) bLFcin derivatives it has already been reported that that a minimum length and net positive charge are required in order to exert an appropriate anticancer activity [50]. Expectedly, the short peptides LF11-322 (+5), LF11-316 (+5) and LF11-318 (+7) only induced minor cell death inducing no effect against cancer cells even if the incubation time was extended to 8 h (Fig. 1) or 24 h (data not shown). Partially the low activity might be related to shortness

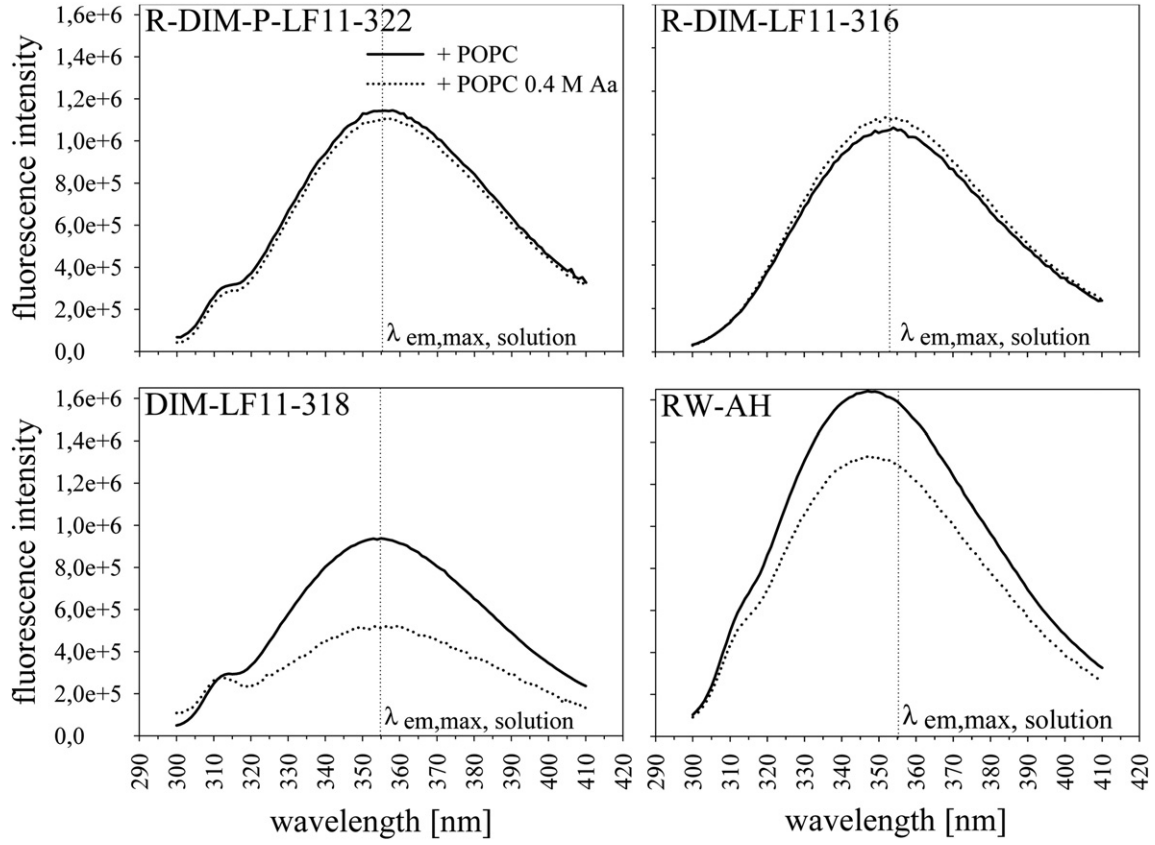

Fig. 6. Tryptophan fluorescence of peptides in the presence of POPC vesicles (small unilamellar vesicles, 100 nm) with buffer or 0.4 M quencher acrylamide (Aa) enclosed. For detection of potential interaction of respective peptides with, respectively penetration of, POPC membranes, tryptophan fluorescence was measured at an excitation wavelength of 280 nm. Dotted vertical line represents $\lambda_{em,\,max}$ of peptides in the presence of the buffer. Curved lines represent wavelength scans of peptides in the presence of POPC vesicles (solid line) and POPC vesicles enclosing 0.4 M acrylamide (dotted line).

and hence potentially lower serum stability [31]. In contrast derivatives exhibiting higher net charges, such as the di-(retro)-peptides R-DIM-P-LF11-322 (+9), R-DIM-LF11-316 (+9), R-DIM-LF11-337 (+13) and DIM-LF11-318 (+13) and the synthetic peptide RW-AH (+10) exhibited highly increased activity against cancer cells of the skin, brain and soft tissue. However the different peptides seem to act via different mechanisms, since the peptides DIM-LF11-318 and RW-AH killed significantly faster than the di-peptides R-DIM-LF11-322 and R-DIM-LF11-316. Strikingly the faster killing properties were not only found to be toxic for cancer but also for differentiated cells like melanocytes or dermal fibroblasts. The different time dependence of cell killing by the peptides indicates two different killing mechanisms as described for other host defense peptides which mainly trigger cell death by necrosis or by induction of apoptosis [7,11]. For triggering necrosis peptides directly kill by disrupting the target plasma membrane, a fast process, whereas for triggering apoptosis they have to enter the cell to reach e.g. a mitochondrial target [11]. The fast activity of RW-AH and DIM-LF11-318 gives strong evidence for a direct membranolytic effect causing necrosis. Structural analysis through CD spectroscopy of DIM-LF11-318 reveals induction of a mostly α-helical structure in the presence of the cancer as well as the non-cancer mimic which might also result in non-selective lyses of cells. The selective peptides R-DIM-P-LF11-322 and R-DIM-LF11-316 obviously act via a different mechanism. The relatively slow action combined with the observation of membrane blebbing is an indication for membrane-mediated apoptosis. This assumption was further proven by caspase-3/7 cleavage studies and an apoptotic DNA-fragmentation assay. Indeed, melanoma cells like SBcl-2 showed activation of caspase-3/7 and DNA fragmentation after incubation with rather low concentrations of R-DIM-P-LF11-322. For induction of apoptosis probably the peptide has to enter the cell specifically via the PS exposing sites (PS-domains) on the surface of cancer cells and further reach negatively charged targets on the surface of cancer cell mitochondria, like phosphatidylserine and cardiolipin. Just previously it has been shown that the LF11 derived peptides not only interact with phosphatidylserine, but also with cardiolipin [40]. Successive swelling of mitochondria and release of cytochrome-C activate the caspase dependent pathway of the programmed cell death. Apoptosis is reported to be blocked in many cancer types as in melanoma cells by inhibition of a gene encoding Apaf-1, the apoptotic protease activating factor-1 [41] or in B-cell-leukemia by expression of high levels of Bcl-2, a protein that blocks apoptotic signals [51]. Induction of apoptosis in human leukemia was also observed for bovine LFcin by Mader et al. [52] and is probably one of the keys for specific anticancer activity of host defense peptides. However, the activity of the original human host defense peptide (hLFcin) is rather low, whereas derived peptides R-DIM-LF11-322 and R-DIM-LF11-316 show significantly increased activities against melanoma and glioblastoma cell lines. Interestingly R-DIM-P-LF11-322 shows an increase in the predominant β-sheet structure in the presence of the cancer mimic and no changes in structure in the presence of the non-cancer cell mimic. So far, most studies report about the necessity of membrane active peptides of formation of an α-helical structure [53,54]. However, in our studies we could show that only the peptide derivatives forming a loop structure separating 2 β-strands or 2 α-helices were able to act specifically on cancer cells without displaying any cytotoxicity on normal cells. Similarly it has been reported recently that membrane-induced folding of the peptide SVS-1 is driven by electrostatic interaction between the peptide and the negatively charged membrane surface

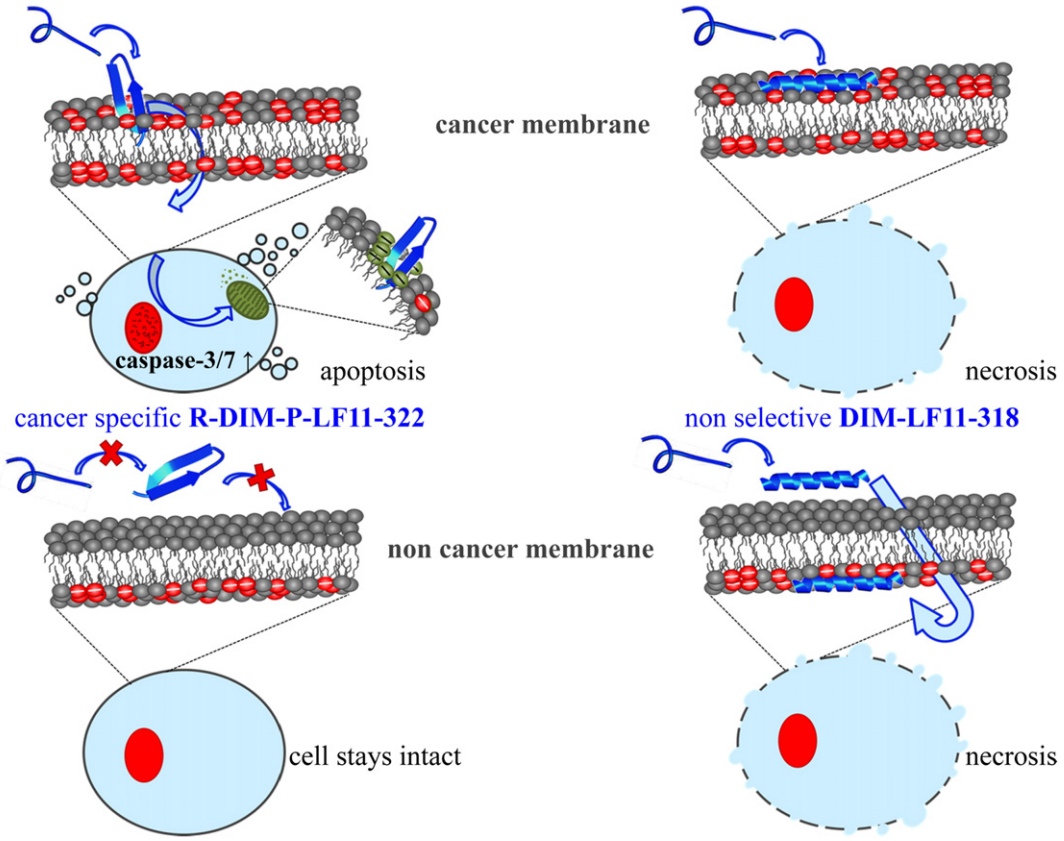

Fig. 7. Proposed mode of action of cancer selective peptide R-DIM-P-LF11-322 (left) and non-selective peptide DIM-LF11-318 (right) with cancer cell membranes (top) and non-cancer cell membranes (bottom) (for description, see the Discussion section).

of cancer cells. The in solution unfolded peptide preferentially folded at the surface of cancer cells, adopting an amphiphilic β-hairpin structure capable of membrane disruption [55].

Since PS is not the only negatively charged interaction partner on the cell surface (for a review see [7]) other cancer cell compounds like sialic residues or heparin or chondroitin sulfate have to be considered. In contrast to PS these molecules however stick out of the membrane, interaction with compounds does therefore not necessarily damage the membrane or enable entrance to the cell. Second these molecules are not specifically present on the surface of cancer cells, but are also present on non-cancer cells. Sialic acid, often increased on the surface of cancer cells, might even protect cancer cells and metastases [56–58] against anticancer drugs, besides being a target for the peptides. It was reported that neuraminidase-treated U937 cells were less susceptible to permeabilization by BMAP peptides, suggesting that the sialyl moieties might be initial interaction sites of these peptides with the cells [33]. In contrast, we could show for several cancer types that cleavage of sialic acid moieties did not significantly change the activity of the studied peptides. The results indicate that the sialic residues are not a main target or initial interaction site, nor a blocker of activity for the peptides studied. Also the metastases WM164 were unaffectedly sensitive to the peptides in the presence of sialic acid and absence thereof. Proteoglycans with highly negatively charged glycosaminoglycan side chains attached to a core protein are also expressed on the cell surface. Two major classes of such side chains are heparan sulfate (HS) and chondroitin sulfate (CS) [14]. HS and/or CS present on cancer and non-cancer cells can be either decreased or increased on cancer cells depending on cancer type [7]. HS and CS thus may be able to act like a protection shield on the surface of cells (cancer and non-cancer), since they protrude out of the cell membrane like a brush [59,60], modulating cell phenotype, growth kinetics, invasiveness and metastatic potential [61–63]. Wade et al. [64] reported for glioblastoma (GBM) a significant up-regulation of many proteoglycans with differences in the tumor subtypes. Also for melanoma an up-regulation of certain glycosaminoglycans was observed [65]. Fadnes et al. [14] found that the anticancer activity of bovine LFcin was inhibited by heparan sulfate on the surface of tumor cells. In our studies the di-peptides derived from hLFcin were however not influenced in their activity by exogenous heparin or chondroitin sulfate at physiological concentrations of 1–10 μg/ml [66,67]. Thus neither heparin nor CS, which is increased on the surface of melanoma cells, seems to significantly protect the cell from the interaction with the studied di-peptides. Interestingly the activity of

Table 3
Influence of sialic acid cleavage from rhabdomyosarcoma cell line TE671 on cytotoxic activity of peptides after 1 h of incubation and melanoma cell lines WM164, A375 and glioblastoma cell line U-87mg after 8 h of incubation with 20 μM peptides.

	PI-uptake [%]	
	Untreated TE671	Sialidase treated TE671
LF11-322	6.1 ± 5.1	4.3 ± 5.0
	Untreated WM164	Sialidase treated WM164
R-DIM-P-LF11-322	36.6 ± 7.7	39.8 ± 16.9
LF11-318	27.0 ± 7.1	32.2 ± 16.0
DIM-LF11-318	67.5 ± 5.6	70.5 ± 18.0
	Untreated A375	Sialidase treated A375
LF11-322	5.4 ± 4.5	13.1 ± 4.8
R-DIM-P-LF11-322	95.2 ± 3.2	93.6 ± 1.9
LF11-318	24.0 ± 14.1	17.8 ± 2.5
DIM-LF11-318	92.3 ± 7.5	89.3 ± 4.3
	Untreated U-87mg	Sialidase treated U-87mg
LF11-322	23.0 ± 6.5	24.5 ± 1.8
R-DIM-P-LF11-322	81.4 ± 10.2	90.7 ± 2.9
LF11-318	21.0 ± 5.9	25.4 ± 3.6
DIM-LF11-318	88.9 ± 6.0	99.7 ± 0.5

Table 4
Influence of heparin and chondroitin sulfate on peptide activity against melanoma cell line A375 after 8 h of incubation with 20 μM peptides.

	PI-uptake [%]				
	A375	+1 μg/ml Heparin	+10 μg/ml Heparin	+1 μg/ml CS	+10 μg/ml CS
LF11-322	5.4 ± 4.5	20.4 ± 8.2	14.5 ± 1.7	22.2 ± 4.1	16.0 ± 2.4
R-DIM-P-LF11-322	95.2 ± 3.2	98.4 ± 1.2	94.4 ± 2.2	99.3 ± 0.7	96.4 ± 1.7
LF11-318	24.0 ± 14.1	52.8 ± 6.5	42.6 ± 10.7	45.2 ± 15.6	44.4 ± 6.6
DIM-LF11-318	92.3 ± 7.5	100.0 ± 0.0	99.7 ± 0.4	100.0 ± 0.0	100.0 ± 0.0

the short peptides, which are under normal conditions only minor active, was however increased by the exogenous addition of heparin and CS. Similarly a contribution of heparan sulfate proteoglycans to the cell entry mechanism of e.g. cell penetrating peptides has been discussed [48]. The short peptides might probably be stabilized by binding to exogenous heparin.

We are proposing different scenarios based on the observed structural properties (Fig. 7). In the presence of cancer membranes cancer specific peptides (as R-DIM-P-LF11-322) adopt a loop structure (CD, PEP-FOLD), interact (only) with negatively charged membrane surfaces (zeta potential and PI-uptake with or without Ca^{2+}), presumably exposed PS [13] (cancer mimic PS, leakage and DSC). They are able to neutralize the negatively charged surface and compete with cations such as Ca^{2+}. However after 8 h and at elevated concentrations they have reached an inner target, probably mitochondria to induce apoptotic killing (apoptosis studies and PI toxicity), membrane blebbing and membrane disintegration occurs, cancer cells die. In case of cell membranes from differentiated cells no change of structure (CD) and no interaction with the neutral surface of normal cells occurs (non-cancer mimic PC, zeta potential), therefore cells stay intact.

Differently non-selective peptides (as DIM-LF11-318) form an α-helical structure in the presence of the cancer and the non-cancer membrane (CD) without a loop (PEP-FOLD). When they contact the cancer membrane they can attach to negatively charged surfaces as PS and/or neutral surfaces as PC and cause fast killing by membrane lyses, presumably by necrosis. The interaction of the α-helical peptide (CD) with non-cancer membranes however does not occur via membrane lyses from the outside (non-cancer mimic PC), but via cell penetration (PC studies with quencher) and then presumably via induction of necrosis (lyses) from the inside of the plasma membrane. This is comparable to the described uptake mechanism of so called cell penetrating peptides [68,69].

In summary our studies provide evidence that specific activity of hLFcin derived peptides depends on a slow killing mechanism, as e.g. apoptosis, rather than killing by necrosis, interaction with PS exposed by cancer cells, not with PC abundant on all cell types, adoption of a β-sheet structure in the presence of cancer cells and no changes in structure in the presence of the non-cancer cell mimic.

Acknowledgments

We thank Sabine Tumer for the technical support.

References

[1] D.S. Shewach, R.D. Kuchta, Introduction to cancer chemotherapeutics, Chem. Rev. 109 (2009) 2859–2861.
[2] D. Schadendorf, M. Worm, B. Algermissen, C.M. Kohlmus, B.M. Czarnetzki, Chemosensitivity testing of human malignant melanoma. A retrospective analysis of clinical response and in vitro drug sensitivity, Cancer 73 (1994) 103–108.
[3] H. Helmbach, E. Rossmann, M.A. Kern, D. Schadendorf, Drug-resistance in human melanoma, Int. J. Cancer 93 (2001) 617–622.
[4] F. Hodi, S. Lee, D. McDermott, U. Rao, L. Butterfield, A. Tarhini, et al., Ipilimumab plus sargramostim vs ipilimumab alone for treatment of metastatic melanoma: a randomized clinical trial, JAMA 312 (2014) 1744–1753.
[5] P.M. Black, Brain tumors, N. Engl. J. Med. 324 (1991) 1555–1564.
[6] J. Skog, T. Wurdinger, S. van Rijn, D.H. Meijer, L. Gainche, M. Sena-Esteves, et al., Glioblastoma microvesicles transport RNA and proteins that promote tumour growth and provide diagnostic biomarkers, Nat. Cell Biol. 10 (2008) 1470–1476.
[7] S. Riedl, D. Zweytick, K. Lohner, Membrane-active host defense peptides — challenges and perspectives for the development of novel anticancer drugs, Chem. Phys. Lipids 164 (2011) 766–781.
[8] D.W. Hoskin, A. Ramamoorthy, Studies on anticancer activities of antimicrobial peptides, Biochim. Biophys. Acta 1778 (2008) 357–375.
[9] J.S. Mader, D.W. Hoskin, Cationic antimicrobial peptides as novel cytotoxic agents for cancer treatment, Expert Opin. Investig. Drugs 15 (2006) 933–946.
[10] F. Schweizer, Cationic amphiphilic peptides with cancer-selective toxicity, Eur. J. Pharmacol. 625 (2009) 190–194.
[11] N. Papo, Y. Shai, Host defense peptides as new weapons in cancer treatment, Cell. Mol. Life Sci. 62 (2005) 784–790.
[12] S.K. Bhutia, T.K. Maiti, Targeting tumors with peptides from natural sources, Trends Biotechnol. 26 (2008) 210–217.
[13] S. Riedl, B. Rinner, M. Asslaber, H. Schaider, S. Walzer, A. Novak, et al., In search of a novel target — phosphatidylserine exposed by non-apoptotic tumor cells and metastases of malignancies with poor treatment efficacy, Biochim. Biophys. Acta 1808 (2011) 2638–2645.
[14] B. Fadnes, O. Rekdal, L. Uhlin-Hansen, The anticancer activity of lytic peptides is inhibited by heparan sulfate on the surface of the tumor cells, BMC Cancer 9 (2009) 183.
[15] T. Utsugi, A.J. Schroit, J. Connor, C.D. Bucana, I.J. Fidler, Elevated expression of phosphatidylserine in the outer membrane leaflet of human tumor cells and recognition by activated human blood monocytes, Cancer Res. 51 (1991) 3062–3066.
[16] L.V. Rao, J.F. Tait, A.D. Hoang, Binding of annexin V to a human ovarian carcinoma cell line (OC-2008). Contrasting effects on cell surface factor VIIa/tissue factor activity and prothrombinase activity, Thromb. Res. 67 (1992) 517–531.
[17] H. Woehlecke, A. Pohl, N. Alder-Baerens, H. Lage, A. Herrmann, Enhanced exposure of phosphatidylserine in human gastric carcinoma cells overexpressing the half-size ABC transporter BCRP (ABCG2), Biochem. J. 376 (2003) 489–495.
[18] M. Cichorek, K. Kozlowska, J.M. Witkowski, M. Zarzeczna, Flow cytometric estimation of the plasma membrane diversity of transplantable melanomas, using annexin V, Folia Histochem. Cytobiol. 38 (2000) 41–43.
[19] D. Zweytick, S. Riedl, B. Rinner, M. Asslaber, H. Schaider, S. Walzer, et al., In search of new targets — the membrane lipid phosphatidylserine — the underestimated Achilles' heel of cancer cells, Ann. Oncol. 22 (Suppl. 3) (2011) iii42–iii43.
[20] H. Schröder-Borm, R. Bakalova, J. Andrä, The NK-lysin derived peptide NK-2 preferentially kills cancer cells with increased surface levels of negatively charged phosphatidylserine, FEBS Lett. 579 (2005) 6128–6134.
[21] E.M. Bevers, P. Comfurius, R.F. Zwaal, Regulatory mechanisms in maintenance and modulation of transmembrane lipid asymmetry: pathophysiological implications, Lupus 5 (1996) 480–487.
[22] R.F. Zwaal, A.J. Schroit, Pathophysiologic implications of membrane phospholipid asymmetry in blood cells, Blood 89 (1997) 1121–1132.
[23] E.M. Bevers, P. Comfurius, D.W. Dekkers, M. Harmsma, R.F. Zwaal, Regulatory mechanisms of transmembrane phospholipid distributions and pathophysiological implications of transbilayer lipid scrambling, Lupus 7 (Suppl. 2) (1998) S126–S131.
[24] M. Seigneuret, P.F. Devaux, ATP-dependent asymmetric distribution of spin-labeled phospholipids in the erythrocyte membrane: relation to shape changes, Proc. Natl. Acad. Sci. U. S. A. 81 (1984) 3751–3755.
[25] C. Kirszberg, L.G. Lima, Da Silva dO, W. Pickering, E. Gray, T.W. Barrowcliffe, et al., Simultaneous tissue factor expression and phosphatidylserine exposure account for the highly procoagulant pattern of melanoma cell lines, Melanoma Res. 19 (2009) 301–308.
[26] J. Connor, C. Bucana, I.J. Fidler, A.J. Schroit, Differentiation-dependent expression of phosphatidylserine in mammalian plasma membranes: quantitative assessment of outer-leaflet lipid by prothrombinase complex formation, Proc. Natl. Acad. Sci. U. S. A. 86 (1989) 3184–3188.
[27] J.L. Gifford, H.N. Hunter, H.J. Vogel, Lactoferricin: a lactoferrin-derived peptide with antimicrobial, antiviral, antitumor and immunological properties, Cell. Mol. Life Sci. 62 (2005) 2588–2598.
[28] D. Zweytick, G. Pabst, P.M. Abuja, A. Jilek, S.E. Blondelle, J. Andrä, et al., Influence of N-acylation of a peptide derived from human lactoferricin on membrane selectivity, Biochim. Biophys. Acta 1758 (2006) 1426–1435.
[29] D. Zweytick, S. Tumer, S.E. Blondelle, K. Lohner, Membrane curvature stress and antibacterial activity of lactoferricin derivatives, Biochem. Biophys. Res. Commun. 369 (2008) 395–400.
[30] D. Zweytick, G. Deutsch, J. Andrä, S.E. Blondelle, E. Vollmer, R. Jerala, et al., Studies on lactoferricin derived *E. coli* membrane active peptides reveal differences in the

mechanism of N-acylated versus non-acylated peptides, J. Biol. Chem. 24 (2011) 21266–21276.
[31] S. Riedl, B. Rinner, H. Schaider, K. Lohner, D. Zweytick, Killing of melanoma cells and their metastases by human lactoferricin derivatives requires interaction with the cancer marker phosphatidylserine, BioMetals 27 (2014) 981–997.
[32] S.A. Rosenberg, A.B. Einstein Jr., Sialic acids on the plasma membrane of cultured human lymphoid cells. Chemical aspects and biosynthesis, J. Cell Biol. 53 (1972) 466–473.
[33] A. Risso, M. Zanetti, R. Gennaro, Cytotoxicity and apoptosis mediated by two peptides of innate immunity, Cell. Immunol. 189 (1998) 107–115.
[34] L. Whitmore, B.A. Wallace, DICHROWEB, an online server for protein secondary structure analyses from circular dichroism spectroscopic data, Nucleic Acids Res. 32 (2004) W668–W673.
[35] L. Whitmore, B.A. Wallace, Protein secondary structure analyses from circular dichroism spectroscopy: methods and reference databases, Biopolymers 89 (2008) 392–400.
[36] N. Sreerama, R.W. Woody, Estimation of protein secondary structure from circular dichroism spectra: comparison of CONTIN, SELCON, and CDSSTR methods with an expanded reference set, Anal. Biochem. 287 (2000) 252–260.
[37] G.R. Bartlett, Colorimetric assay methods for free and phosphorylated glyceric acids, J. Biol. Chem. 234 (1959) 469–471.
[38] R.M. Broekhuyse, Phospholipids in tissues of the eye. I. Isolation, characterization and quantitative analysis by two-dimensional thin-layer chromatography of diacyl and vinyl-ether phospholipids, Biochim. Biophys. Acta 152 (1968) 307–315.
[39] W. Jing, E.J. Prenner, H.J. Vogel, A.J. Waring, R.I. Lehrer, K. Lohner, Headgroup structure and fatty acid chain length of the acidic phospholipids modulate the interaction of membrane mimetic vesicles with the antimicrobial peptide protegrin-1, J. Pept. Sci. 11 (2005) 735–743.
[40] D. Zweytick, B. Japelj, E. Mileykovskaya, M. Zorko, W. Dowhan, S.E. Blondelle, et al., N-acylated peptides derived from human lactoferricin perturb organization of cardiolipin and phosphatidylethanolamine in cell membranes and induce defects in *Escherichia coli* cell division, PLoS One 9 (2014) e90228.
[41] M.S. Soengas, P. Capodieci, D. Polsky, J. Mora, M. Esteller, X. Opitz-Araya, et al., Inactivation of the apoptosis effector Apaf-1 in malignant melanoma, Nature 409 (2001) 207–211.
[42] J. Maupetit, P. Derreumaux, P. Tufféry, PEP-FOLD: an online resource for de novo peptide structure prediction, Nucleic Acids Res. 37 (2009) W498–W503.
[43] J. Maupetit, P. Derreumaux, P. Tufféry, A fast method for large-scale de novo peptide and miniprotein structure prediction, J. Comput. Chem. 31 (2010) 726–738.
[44] P. Thévenet, Y. Shen, J. Maupetit, F. Guyon, P. Derreumaux, P. Tufféry, PEP-FOLD: an updated de novo structure prediction server for both linear and disulfide bonded cyclic peptides, Nucleic Acids Res. 40 (2012) W288–W293.
[45] D.W. Kufe, Mucins in cancer: function, prognosis and therapy, Nat. Rev. Cancer 9 (2009) 874–885.
[46] K.L. Carraway, S.A. Price-Schiavi, X. Zhu, M. Komatsu, Membrane mucins and breast cancer, Cancer Control 6 (1999) 613–614.
[47] S. Bafna, S. Kaur, S.K. Batra, Membrane-bound mucins: the mechanistic basis for alterations in the growth and survival of cancer cells, Oncogene 29 (2010) 2893–2904.
[48] M. Belting, Heparan sulfate proteoglycan as a plasma membrane carrier, Trends Biochem. Sci. 28 (2003) 145–151.
[49] S. Ran, P.E. Thorpe, Phosphatidylserine is a marker of tumor vasculature and a potential target for cancer imaging and therapy, Int. J. Radiat. Oncol. Biol. Phys. 54 (2002) 1479–1484.
[50] N. Yang, M.B. Strom, S.M. Mekonnen, J.S. Svendsen, O. Rekdal, The effects of shortening lactoferrin derived peptides against tumour cells, bacteria and normal human cells, J. Pept. Sci. 10 (2004) 37–46.
[51] T. Miyashita, J.C. Reed, Bcl-2 oncoprotein blocks chemotherapy-induced apoptosis in a human leukemia cell line, Blood 81 (1993) 151–157.
[52] J.S. Mader, J. Salsman, D.M. Conrad, D.W. Hoskin, Bovine lactoferricin selectively induces apoptosis in human leukemia and carcinoma cell lines, Mol. Cancer Ther. 4 (2005) 612–624.
[53] Huang Yb, Wang Xf, Wang Hy, Y. Liu, Y. Chen, Studies on mechanism of action of anticancer peptides by modulation of hydrophobicity within a defined structural framework, Mol. Cancer Ther. 10 (2011) 416–426.
[54] L.T. Eliassen, B.E. Haug, G. Berge, O. Rekdal, Enhanced antitumour activity of 15-residue bovine lactoferricin derivatives containing bulky aromatic amino acids and lipophilic N-terminal modifications, J. Pept. Sci. 9 (2003) 510–517.
[55] C. Sinthuvanich, A.S. Veiga, K. Gupta, D. Gaspar, R. Blumenthal, J.P. Schneider, Anticancer β-hairpin peptides: membrane-induced folding triggers activity, J. Am. Chem. Soc. 134 (2012) 6210–6217.
[56] F.L. Wang, S.X. Cui, L.P. Sun, X.J. Qu, Y.Y. Xie, L. Zhou, et al., High expression of alpha 2, 3-linked sialic acid residues is associated with the metastatic potential of human gastric cancer, Cancer Detect. Prev. 32 (2009) 437–443.
[57] A. Litynska, M. Przybylo, E. Pochec, D. Hoja-Lukowicz, D. Ciolczyk, P. Laidler, et al., Comparison of the lectin-binding pattern in different human melanoma cell lines, Melanoma Res. 11 (2001) 205–212.
[58] A. Cazet, S. Julien, M. Bobowski, M.A. Krzewinski-Recchi, A. Harduin-Lepers, S. Groux-Degroote, et al., Consequences of the expression of sialylated antigens in breast cancer, Carbohydr. Res. 345 (2010) 1377–1383.
[59] R. Sasisekharan, Z. Shriver, G. Venkataraman, U. Narayanasami, Roles of heparan-sulphate glycosaminoglycans in cancer, Nat. Rev. Cancer 2 (2002) 521–528.
[60] R.D. Sanderson, Heparan sulfate proteoglycans in invasion and metastasis, Semin. Cell Dev. Biol. 12 (2001) 89–98.
[61] D.F. Liu, Z. Shriver, Y.W. Gi, G. Venkataraman, R. Sasisekharan, Dynamic regulation of tumor growth and metastasis by heparan sulfate glycosaminoglycans, Semin. Thromb. Hemost. 28 (2002) 67–78.
[62] G.W. Yip, M. Smollich, M. Götte, Therapeutic value of glycosaminoglycans in cancer, Mol. Cancer Ther. 5 (2006) 2139–2148.
[63] M.M. Fuster, J.D. Esko, The sweet and sour of cancer: glycans as novel therapeutic targets, Nat. Rev. Cancer 5 (2005) 526–542.
[64] A. Wade, A.E. Robinson, J.R. Engler, C. Petritsch, C.D. James, J.J. Phillips, Proteoglycans and their roles in brain cancer, FEBS J. 280 (2013) 2399–2417.
[65] T.F.C.M. Smetsers, E.M.A. Van de Westerlo, G.B. ten Dam, R. Clarijs, E.M.M. Versteeg, W.L. van Geloof, et al., Localization and characterization of melanoma-associated glycosaminoglycans: differential expression of chondroitin and heparan sulfate epitopes in melanoma, Cancer Res. 63 (2003) 2965–2970.
[66] H. Engelberg, Plasma heparin levels in normal man, Circulation 23 (1961) 578–581.
[67] N. Volpi, M. Cusmano, T. Venturelli, Qualitative and quantitative studies of heparin and chondroitin sulfates in normal human plasma, Biochim. Biophys. Acta 1243 (1995) 49–58.
[68] F. Madani, S. Lindberg, Ü. Langel, S. Futaki, A. Grälund, Mechanisms of cellular uptake of cell-penetrating peptides, J. Biophys. 2014 (2011).
[69] M. Zorko, Ü. Langel, Cell-penetrating peptides: mechanism and kinetics of cargo 1delivery, Adv. Drug Deliv. Rev. 57 (2005) 529–545.